# Role of Chain Architecture in the Adhesion of Block Copolymers

**Afshin Falsafi,* Frank S. Bates, and Matthew Tirrell†**

*Department of Chemical Engineering and Materials Science, University of Minnesota, Minneapolis, Minnesota 55455*

*Received February 4, 2000; Revised Manuscript Received September 18, 2000*

ABSTRACT: We have used Johnson−Kendall−Roberts contact mechanics methodology to study the self-adhesion of block copolymers. The block copolymers studied contain building blocks that have different physical states as well as different dynamic characteristics. The polymers chosen are poly(styrene)−poly(isoprene) (PS−PI), poly(styrene)−poly(ethylethylene) (PS−PEE) diblocks and PS−PI−PS, PS−PEE−PS triblocks that have the tail and looped chain surface architectures, respectively. Our results for unloading of the diblock/triblock mixtures, where two surfaces are separated by decreasing the amount of compression, show a maximum in adhesion vs mixture composition when the contact time is short. For contact times longer than 30 min, only unloading of triblock-dominated mixtures shows considerable buildup of adhesion with time. The surface energies obtained from loading experiments do not show any detectable influence of chain architecture on the thermodynamic work of adhesion.

## 1. Introduction

Self-assembly of block copolymers provides adhesion scientists and engineers with new routes to study and design model interfaces. Block copolymers are composed of several chemically dissimilar components that are generally incompatible. These unfavorable interactions are the driving force for macrophase separation observed in polymer blends. However, since the dissimilar blocks are covalently linked into a single chain, the microdomain size is bound to a macromolecular scale. The resulting *mesophases* exhibit space-filling features similar to those of crystalline materials and conform to the same principles of symmetry ordering.[1−5] The mechanical and physical properties of this potentially anisotropic class of polymers are influenced by the shape of filling structures and the adopted symmetry. The configuration of the surface-active block (usually the one with the lowest surface energy) is another interesting characteristic of these materials. The so-called *surface architectures* could dominate the interfacial response of these materials to their boundaries. The ordering process in a film of block copolymers confined to at least one soft (deformable) boundary is also accompanied by the development of a surface *topology* known as "islands and holes". This means that different regions of film may assume different values but multiple of a periodic thickness known as domain spacing *d*.

In the work presented here, we have extended the JKR methodology to adhesion measurements of intrinsically viscoelastic block copolymers. Polymeric layers were prepared and supported on elastic, surface-treated cross-linked PDMS caps to remove bulk viscoelastic effects. Our previous study on the adhesion of PE−PEP diblock copolymers has shown that even for the loading (crack healing) experiments the bulk viscoelastic effects cannot be ignored.[6]

The building blocks of our copolymers, shown in Table 1, have different physical states at room temperature with different dynamic characteristics. We compared the dynamics of disentanglement for diblock "chains" and triblock "loops" as depicted in Figure 1. Simulation studies on mixtures of surface-grafted looped chains and tails suggest that the static conformational properties are comparable to those of bidisperse mixtures of grafted tails that differ in length by a factor of 2.[9] The phase diagram of triblocks has also been shown to be similar to that of the homologous diblocks after accounting for a doubling of the molecular weight in the mean-field theories.[2]

**Table 1. Molecular Characteristics of Polymers Studied**

| polymer | $T_g$,[d] °C | $M_e$,[e] g/mol | $\gamma_s$,[f] mJ/m$^2$ |
|---|---|---|---|
| PS | 100 | 13 500 | 44[a] |
| PEE | −20 | 12 200 | 29[b] |
| PI | −70 | 5097 | 33[c] |

[a] Reported value in ref 7. [b] Measured surface energy in ref 17. [c] Measured surface energy in this study. [d] Glass transition temperature. [e] Molecular weight between entanglements.[8] [f] Surface energy.

## 2. Experimental Methods

**Preparation of Layered Samples.** The layered samples were made in the following order:

(a) The polymer was dissolved in toluene to make a 3% solution (w/w). The solution was precipitated in methanol three times to remove impurities. The precipitated polymer was dried and dissolved in an appropriate solvent to the desired concentration. The final solution was filtered using 0.2 $\mu$m PTFE filters. The final concentration range is 1−3% depending on the polymer used and the desired layer thickness.

(b) The prepared polymer solutions were spun-cast ($\nu$ = 500−3000 rpm) onto freshly cleaved/rinsed mica sheets. The spinning times were generally 2 min.

(c) The polymer-coated mica sheets were annealed under 0.05 mbar vacuum. The temperature was raised to 140 °C (between the glass transition temperature $T_g$ and the order−disorder transition $T_{ODT}$) so that the desired cylindrical microstructure was developed. The samples were annealed at this temperature for at least 6 h. The temperature was lowered to room temperature by simply turning the oven off while the vacuum was in effect.

(d) The annealed polymer-coated mica sheets were cut in small pieces (1 cm × 3 cm) and rinsed with deionized (DI) water to remove any mica debris prior to dipping in a dish containing DI water. The dipping was performed by slowly

* To whom correspondence should be addressed. Current address: 3M Dental Products Laboratory, St. Paul, MN 55144.

† Current address: College of Engineering, University of California, Santa Barbara, CA 93106.

10.1021/ma0002085 CCC: $20.00 
Published on Web 01/25/2001

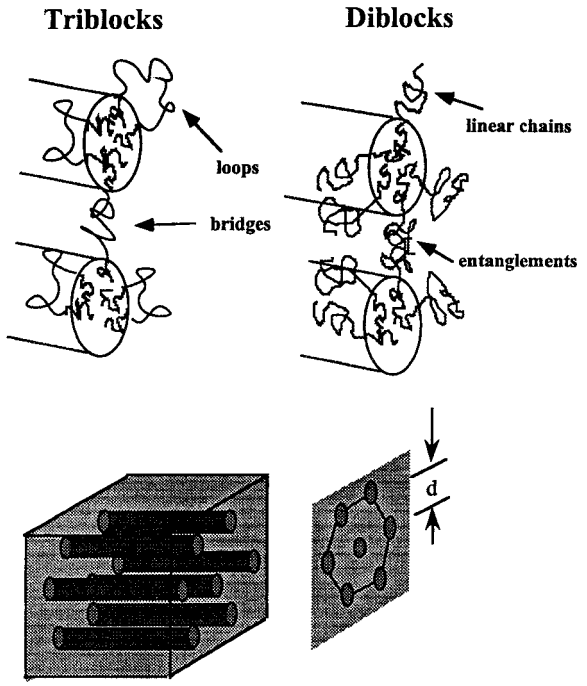


**Figure 1.** Illustration of block copolymer morphology and chain architecture. *d* is the domain spacing for the hexagonally packed cylinders.

inserting the mica piece in the DI water at a small angle. This allowed gradual migration of water to the polymer/mica interface and final detachment and flotation of the film without any folding and excessive stretching. The floated polymer was picked up by a treated PDMS cap (see next section) supported on a small piece of silicon wafer. The polymer-coated PDMS caps were left for 3 h to dry slowly. Finally, and most importantly, the coated caps were placed in a vacuum oven at 65 °C for 30 min to complete the drying process and to establish a reinforced interface between the polymer film and the treated PDMS cap (through possible interdiffusion of chains). Excess film on the silicon was used for determining film thickness and/or contact mechanical experiments provided that the silicon wafer had been surface-modified in a similar procedure as the PDMS caps.

**Surface Modification of Cross-Linked PDMS Caps.** The preparation of the cross-linked PDMS caps is reported elsewhwere.[10] The molecular weight between cross-links is approximately 10 000 g mol$^{-1}$, and the functionality of cross-linker is 50. The unreacted PDMS prepolymer and cross-linker were removed from the caps by Soxhlet extraction in fresh heptane for 24 h. The caps were dried under vacuum at 50 °C for 2 h.

(a) The extracted caps were placed in a $H_2O$-plasma chamber for 2 min with argon as the carrier gas. The vacuum inside the chamber was 0.5 mbar, and the plasma power was set at 10 W. The $H_2O$-plasma treatment of the PDMS caps created hydroxyl groups on the surface which could readily react with the silane coupling agent to provide the desired olefin-like surface that was compatible with the surface-active blocks of our studied samples. Therefore, the freshly plasma-treated PDMS caps were dipped for 2 h in a 1% silane solution. The silane solution was made by mixing 20 parts of Dow-Corning Z6032 silane coupling agent (*N*-[2-(vinylbenzylamino)-ethyl]-3-aminopropyltrimethoxysilane, 40% active), 5 parts of DI water, and 1 part of acetic acid glacial. After 1 h of mixing, the 30% active solution was diluted to 1% by adding methanol. The surface-treated caps were rinsed thoroughly with methanol to remove any silanes beyond a monolayer coverage. These caps were baked in a vacuum oven for 2 h at 80 °C to drive the surface reaction to completion.[11]

(b) In order to remove any loose chains that might have been created in the course of plasma treatment, the caps were additionally Soxhlet extracted with heptane for 24 h and subsequently dried at 50 °C under vacuum. The treated PDMS caps were screened for surface smoothness by an optical microscope and used either as elastic substrates for the polymer films or directly as impenetrable surfaces in our adhesion experiments.

Table 2 summarizes the physical and chemical characteristics of the studied samples. The PS−PI and PS−PI−PS samples were kindly donated by D. Handlin from Shell Company to our group for structural analyses.[13] PS−PEE and PS−PEE−PS are commercial Kraton rubbers that were obtained from Shell Company as well.

**Molecular Weight Determinations.** The reported molecular weights of PS−PI and PS−PI−PS are based on reaction stoichiometry and yield in anionic polymerization. Gel permeation chromatography (GPC) traces of the PS−PEE/PS−PEE−PS (70/30, w/w) sample were obtained from a Waters 150C instrument at 25 °C with tetrahydrofuran as the mobile phase at a flow rate of 1 mL/min. Elution times were detected by a differential refractometer following the injection of 0.25 mL of 0.1% (w/w) solution in benzene. Calibration was obtained using a set of PS standards.

**Film Thickness Measurements.** The thickness of films were measured using a Tencor P-10 surface profiler. The vertical and lateral resolutions are 0.1 Å and 2 $\mu$m, respectively, for the stylus with a radius of 5 $\mu$m. A gentle groove was made on the film samples using a needle. The groove was scanned in the perpendicular direction. To investigate the extent of film deformation in contact with stylus, different levels of stylus loads were used. The data expressing film thickness vs stylus load showed a plateau for stylus loads less than 0.5 dyn. In all thickness measurements a stylus load of 0.05 dyn was used.

**Contact Mechanical Measurement of Adhesion.** We have used the Johnson−Kendall−Roberts (JKR) methodology[14] to measure the adhesive properties of our materials. In this methodology, two homogeneous elastic bodies, usually two hemispheres or one hemisphere and one flat, are approached slowly so that an initial contact is established. For the experiments in this study, the following scheme was considered. In the loading part of the experiment approximately 12 steps of compression (~1.5 $\mu$m per step) were imposed, and the resulting load $P$ and contact radius $a$ were monitored. To capture the time-dependent effects and/or equilibrate the contact, each compression was followed by approximately 20 min of rest. After reaching the final compression, $\delta_{max}$, the surfaces were left in contact for another 30 min. During loading and contact time the interface could potentially rearrange and realize its equilibrium state. From this point on, the compression was decreased dynamically in which the surfaces were continuously separated at a constant speed of $d\delta/dt = 10$ nm s$^{-1}$.

The JKR theory gives an expression which relates the cube of contact radius to the applied load $P$:

$$a^3 = \frac{R}{K}(P + 3\pi RG + \sqrt{6\pi RGP + 9\pi^2 R^2 G^2}) \qquad (1)$$

$R = R_1R_2/(R_1 + R_2)$ is the equivalent radius of curvature, $K = 16/18E$ is the elastic constant ($E$ is the Young's modulus), and $G$ is the strain energy release rate, or equivalently the adhesion energy. For the loading part, a two-parameter curve-fitting of the set of ($a^3$, $P$) data gives the best values of $K$ and $G$, while $R$ is measured independently. The calculated $G$ from the loading part corresponds to the intermolecular interactions experienced by the surfaces, namely the thermodynamic work of adhesion, $W$. For the unloading part, $G$ has contributions from the interface, its dynamic processes, and bulk viscoelasticity. Equation 1 can be rearranged to evaluate $G$ in unloading experiments as

$$G = \frac{(Ka^3/R - P)^2}{6\pi Ka^3} \qquad (2)$$

where the value of $K$ calculated from the loading data is used.

**Table 2. Characteristics and Properties of Copolymers Chosen**

| sample | $f_{PS}$[d] | $M_n$, g/mol | $T_{ODT}$,[b] °C | morphology[c] | $d$,[g] nm | thickness, nm |
|---|---|---|---|---|---|---|
| PS−PI | 0.15 | 60 000 | 200 | C | 29 | 55 |
| PS−PI−PS | 0.15 | 120 000 | 225 | C | 29 | 85 |
| PS−PEE[e] | 0.26 | 36 000 | >150 | C[d] | | 155 |
| PS−PEE−PS[f] | 0.26 | 73 000 | >150 | C[d] | 25 | 155 |

[a] Volume fraction of the glassy block. [b] Order−disorder transition temperature. [c] Room temperature morphology, C = hexagonally packed cylinders. [d] The morphology from SAXS on the 1% functionalized polymer.[12] [e] This is Kraton G-1726 from Shell Co. which has 30% matched PS−PEE−PS triblock. [f] This is Kraton G-1652 from Shell Co. [g] Domain spacing in the bulk from SAXS or SANS measurements.

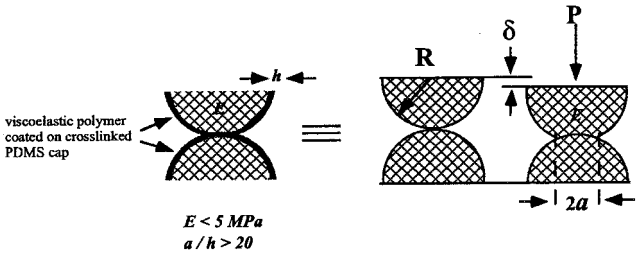


**Figure 2.** Contact mechanical variables in adhesion measurements and the structure of layered samples.

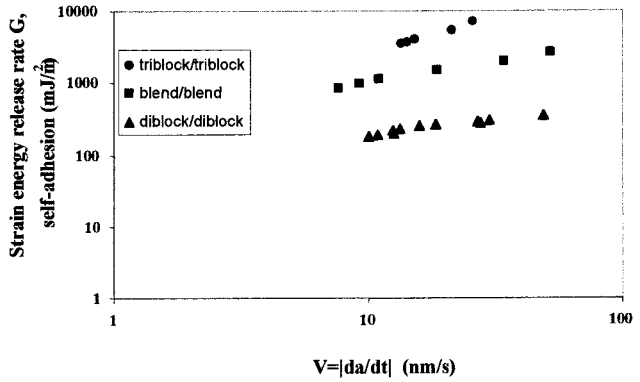


**Figure 3.** Comparison of the unloading dynamics when the same layers of PS−PI diblock, PS−PI−PS triblock, and their 50/50 blend are coated on surface-modified cross-linked PDMS caps.

The JKR theory is a continuum theory in which two elastic semiinfinite bodies are in a nonconforming contact. Recently, the contact of layered solids has been addressed within the framework of the JKR theory.[15] It has been shown that when the substrate modulus is low ($K$ < 5 MPa) and the contact radius-layer thickness ratio is large ($a/h$ > 20), the surface layer will make a negligible contribution to the stiffness of the system, and the layered solid acts as a homogeneous half-space of substrate material while the surface and interfacial properties are governed by those of the layer.[15,16] The extension of the theory to layered bodies has two important implications. First, hard and opaque materials can be coated on soft and clear substrates which deform more readily by small surface forces. Second, viscoelastic materials can be coated on soft elastic substrates, thereby reducing their time-dependent effects. Figure 2 illustrates the contact geometry and sample type used in our adhesion studies. The automated JKR apparatus used in our measurements is fully explained somewhere else.[17] As for our experiments here, the main features of this apparatus are the displacement-controlled loading conditions and the controlled illumination of the samples (light off between the measurements) in order to minimize heating and/or light-sensitive surface reactions.[18]

## 3. Results and Discussion

Figure 4a gives the self-adhesion measurements for the PS−PI/PS−PI−PS blends. The film thickness for the 0/100, 50/50, and 100/0 blends are 85, 75, and 55 nm,

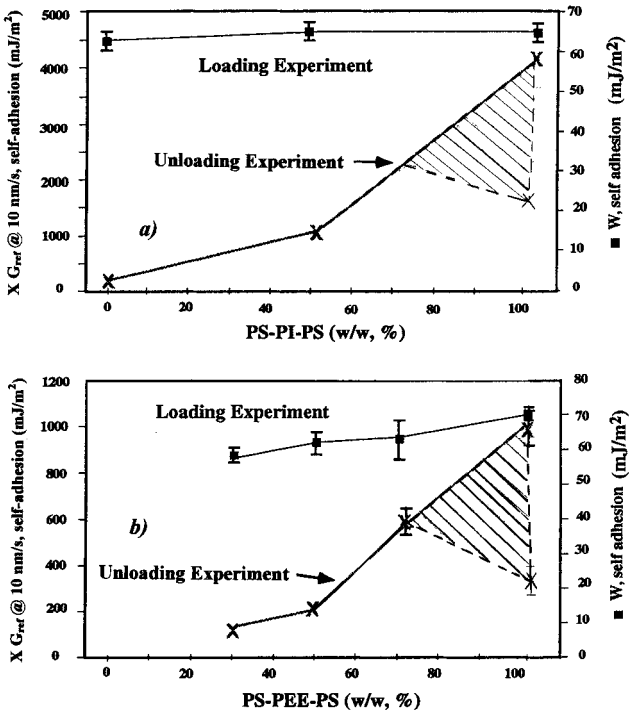


**Figure 4.** Effect of surface architecture on adhesion of matched diblock and triblocks of PS−PI/PS−PI−PS (a) and PS−PEE/PS−PEE−PS (b). $G_{ref}$ is the value of strain energy release rate at 10 nm $s^{-1}$ for crack propagation speed. Square symbols refer to the thermodynamic work of adhesion values obtained from loading experiments. The crosses represent the unloading data. The self-adhesion energies for unloading are influenced by diblock/triblock mixing. The values of thermodynamic work of adhesion are not affected by diblock/triblock mixing. The shaded areas are meant to illustrate the adhesion buildup (crack welding process, described in text and Figure 5) in triblock-dominant mixtures of diblocks and triblocks. The data points are the average value of two or more measurements. Error bars correspond to the errors involved in each measurement (obtained from the uncertainties in load, contact radius, and cap radius measurements as well as the amplitude of fluctuations due to the stick-and-slip nature of unloading experiments) divided by the root square of number of times the data point was generated.

respectively. The values of thermodynamic work of adhesion ($W = 2\gamma_{PI} = 65 \pm 2$ mJ $m^{-2}$) from the loading curves do not seem to depend on the diblock/triblock mixing. However, there is a difference between the dynamics of separation of the diblocks and the triblocks indicated by the values of $G$ in Figure 3. $G_{ref}$ in Figure 4 is the strain energy release rate (from eq 2) at the reference crack growth speed of 10 nm $s^{-1}$. From our previous studies, we have found $V_{ref} \equiv -da/dt \approx 10$ nm $s^{-1}$ to be low enough to reflect the dynamics of the interface with minimum contribution from viscoelastic losses in the bulk samples.[17] Here, we have chosen the same value for $V_{ref}$ which is almost the lowest accessible

speed after the initiation and subsequent propagation of the crack. Another feature is the great influence of contact time on the self-healing of samples where the triblock is the dominant component. The same observations were made for the PS−PEE/PS−PEE−PS system as shown in Figure 4b, though the value of $W = 2\gamma_{PEE}$ is slightly higher than our previous measurements.[17] The film thickness values for the 0/100, 30/70, 50/50, and 70/30 PS−PEE/PS−PEE−PS blends are 155, 135, 160, and 155 nm, respectively. In Figure 4a,b there are two adhesion energy values reported for PS−PI−PS and PS−PEE−PS samples during unloading. The lower value for each of these two samples was the lowest adhesion energy measured for that sample based on a cumulative contact time of approximately 30 min. The other points on these figures correspond to cumulative contact times after which there was no more enhancement in adhesion provided that the final $G$ was below its experimental limit corresponding to the failure of film/supporting cap interface. (The failure is usually accompanied by a fast relief of tension and is evidenced by the image of the peeled-off contact area after complete separation of the surfaces.) Such contact times were found to be less than 30 min for all contacts excluding those for triblock self-adhesion.

The reproducible values of surface energies from the loading parts of the JKR plots obtained for surface-active PI and PEE blocks from Figures 4a,b support the applicability of the JKR methodology in our adhesion measurements, even when the samples are made by coating a thin layer (less than 1 $\mu$m) of viscoelastic polymer on surface-modified cross-linked PDMS substrates. The absence of long-term time-dependent behavior (greater than a few minutes) for contact between such layers in loading mode shows that the time-dependent behavior seen in adhesion between bulk samples is governed by viscoelastic effects. The presence of islands and holes did not result in any loss of adhesion due to surface roughness. This lack of adhesion loss can be attributed to the softness of the films and supporting PDMS caps that could easily deform and conform to the surface topography.

In a systematic study to reveal the contribution of viscoelastic and chain recoiling dissipation[19] upon separation, the layered samples were brought into contact with impenetrable, surface-hydrophobized, cross-linked PDMS caps. The $G_{ref}$ values measured in the unloading experiments were generally a fraction of those values for self-adhesion experiments.[17]

Shorter contact time adhesion data in Figure 4 suggest that there is a maximum for self-adhesion of diblock/triblock mixtures at a certain composition. This is consistent with the Velcro fastener analogy that loop-tail interpenetration reinforces the interface. The asymmetry in adhesion−composition diagrams shows that the interfacial reinforcement is not a "per chain" property.

As mentioned before, the contact time plays an important role in contact between triblocks. Figure 5 shows how molecular processes across the interface *weld* the PS−PEE−PS triblocks with time. We contacted and separated the fresh triblock surfaces twice for a contact time of at least 30 min each prior to any measurements. Further adhesion measurements on such samples for any duration of contact were reproducible. The welding kinetics of triblock interfaces, shown in Figure 5, calls for more attention. Unfortunately, to the best of our knowledge, there are no theoretical means to render quantitative conclusions to determine the mechanism(s) of the interdiffusion process from such adhesion data. However, the time scale involved points out very slow motions. It is noteworthy to mention that the molecular weights of the rubbery blocks in our experiments exceeded several $M_e$.[20]

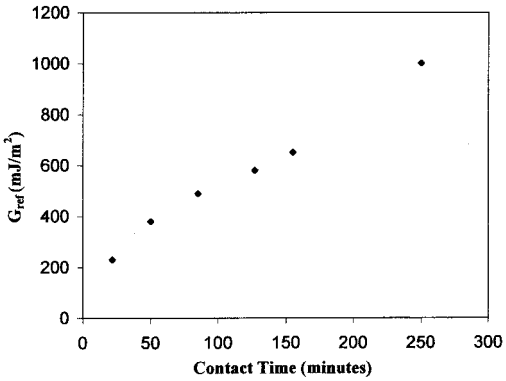


**Figure 5.** Welding of PS−PEE−PS triblocks. The triblocks layers were coated on surface-modified cross-linked PDMS caps. The contact times are cumulative over the loading period and unloading time up to the instant at which the reference crack propagation speed $V_{ref} = 10$ nm s$^{-1}$ was observed.

The above results show that any *morphology−adhesion* relationship should be viewed in the light of *chain architecture* and possibly chain entanglement effects. Though our data suggest self-adhesion of copolymers is affected by chain architecture, it does not rule out the further influence of *surface morphology* on adhesion. For example, the cylindrical morphology in triblocks could provide a "perforated interface" which can be crossed by the opposite side loops for long excursions in the "networks". This situation, known as the "cactus", has been considered for penetration of a "pseudobrush" in a network by Brochard-Wyart et al.[21] Their theoretical results show that the "cactus effect" should not occur for chains longer than the molecular weight between cross-links; otherwise, there would be strong reduction in entropy. The fundamental question to us was whether the loop−network interaction or loop−loop interaction was contributing to the strong self-adhesion of the triblocks.

To address the above question, we brought the PS−PI−PS triblock in contact with the matched PS−PI diblock. Although both polymers adopt a cylindrical morphology at room temperature, the connectivity between the PS cylinders in the diblock is only sustained by entanglements between the PI chains (Figure 1). The observed adhesion was approximately the same as the diblock self-adhesion, and similarly there was no welding kinetics. Therefore, if there were any loop excursions in the diblock layer, upon separating the surfaces it should have caused an extensive amount of viscoelastic dissipation and surface damage (cohesive failure in the diblock layer). The lack of such observations in the triblock against diblock adhesion test suggests that a loop−loop interaction from the opposite sides of the interface is needed to weld the interface. The above argument assumes adhesive failure upon separation of diblocks from triblocks. However, if the mode of failure is indeed a cohesive one occurring within the diblock layer, and additionally, if such a damage could not have been detected optically in our experiments after full separation of surfaces, the loop excursion in the diblock

layer cannot be ruled out.[22] Similar experiments on systems with a "nonperforated surface morphology" such as lamellae can be very useful and complementary to this study.

## 4. Conclusions

The results presented here suggest that the JKR technique can be reliably used to measure the surface energies and dynamics of a variety of viscoelastic polymers when the samples are made by coating thin layers of the polymers on elastic and soft PDMS caps. Our adhesion results show the influence of chain architecture on the self-adhesion of triblocks that cannot be merely explained by chain recoiling and/or viscoelasticity. The results provide a chain architecture−adhesion relationship that accounts for influence of surface architecture on adhesion of block copolymers. The thermodynamic work of adhesion is shown to depend on the chemistry of surface-active block and does not vary with chain architecture, suggesting the minor role of entropic effects.

**Acknowledgment.** The authors thank Nargraj Konerapalli for his pivotal and motivating ideas and help concerning the sample preparation methodology, Al Pocius and Subu Mangipudi (3M) for their valuable insights, and Chang-Yeol Ryu for providing us with the materials. We also thank the Center for Interfacial Engineering, a National Science Foundation research center at the University of Minnesota, for financial support of A.F. and funding of the automated JKR apparatus. Communication with Professor K. L. Johnson on the contact mechanics of layered samples has been very important to us.

## References and Notes

(1) Bates, F. S.; Schulz, M. F.; Khandpur, A. K.; Forster, S.; Rosedale, J. H. *Faraday Discuss. Chem. Soc.* **1994**, *98*, 7.

(2) Gehlsen, M. D.; Almdal, K.; Bates, F. S. *Macromolecules* **1992**, *25*, 939.

(3) Sikka, M.; Singh, N.; Karim, A.; Bates, F. S.; Satija, S. K.; Majkrzak, C. F. *Phys. Rev. Lett.* **1993**, *70*, 307.

(4) Foster, M. D.; Sikka, M.; Singh, N.; Bates, F. S.; Satija, S. K.; Majkrzak, C. F. *J. Chem. Phys.* **1992**, *96*, 8605.

(5) Karim, A.; Singh, N.; Sikka, M.; Bates, F. S.; Dozier, W. D.; Flecher, G. P. *J. Chem. Phys.* **1994**, *100*, 1620.

(6) Falsafi, A.; Deprez, P.; Bates, F. S.; Tirrell, M. *J. Rheol.* **1997**, *41*, 1349.

(7) Mangipudi, V. S. Thesis, University of Minnesota, 1995.

(8) Fetters, L. J.; Lohse, D. J.; Richter, D.; Witten, T. A.; Zirkel, A. *Macromolesules* **1994**, *27*, 4639.

(9) Driscoll, D. C.; Gulati, H. S.; Spontak, R. J.; Hall, C. K. *Polymer* **1998**, *39*, 6339.

(10) Deruelle, M.; Tirrell, M. *Macromolecules* **1995**, *28*, 7419.

(11) Kessel, C. R.; Granick, S. *Langmuir* **1991**, *7*, 532.

(12) Ho, R.-M.; Adedeji, A.; Giles, D. W.; Hajduk, D. A.; Macosko, C. W.; Bates, F. S. *J. Polym. Sci., Part B: Polym. Phys.* **1997**, *35*, 2857.

(13) Ryu, C. Y.; Lee, M. S.; Hajduk, D. A.; Lodge, T. P. *J. Polym. Sci., Part B: Polym. Phys.* **1997**, *35*, 2811.

(14) Johnson, K. L.; Kendall, K.; Roberts, A. D. *Proc. R. Soc. London, Ser. A* **1971**, *324*, 301.

(15) Sridhar, I.; Johnson, K. L.; Fleck, N. A. *J. Phys. D: Appl. Phys.* **1997**, *30*, 1710.

(16) Personal communication with K. L. Johnson.

(17) Falsafi, A. Ph.D. Thesis, University of Minnesota, 1998.

(18) Brown, H. R. *Macromolecules* **1993**, *26*, 1666.

(19) Lake, G. J.; Thomas, A. G. *Proc. R. Soc. London, Ser. A* **1967**, *300*, 108.

(20) Brown, H. R.; Russell, T. P. *Macromolecules* **1996**, *29*, 798.

(21) Brochard-Wyart, F.; de Gennes, P. G.; Leger, L.; Marciano, Y.; Raphael, E. *J. Phys. Chem.* **1994**, *98*, 9405.

(22) The signatures of cohesive failure in our other studied systems (lower molecular weight PS−PI diblocks)[17] have been the observation of the damaged contact area after separation of the surfaces and equal $G$ values in separation of diblocks from diblocks and impenetrable surface-modified PDMS caps.

MA0002085